Molecular Biology of the Cell
Vol. 11, 339–354, January 2000

Functions and Functional Domains of the GTPase Cdc42p

Keith G. Kozminski, Ann J. Chen, Avital A. Rodal, and David G. Drubin*

Department of Molecular and Cell Biology, University of California, Berkeley, California 94720-3202

Submitted September 2, 1999; Revised October 5, 1999; Accepted October 14, 1999
Monitoring Editor: Juan Bonifacino

Cdc42p, a Rho family GTPase of the Ras superfamily, is a key regulator of cell polarity and morphogenesis in eukaryotes. Using 37 site-directed *cdc42* mutants, we explored the functions and interactions of Cdc42p in the budding yeast *Saccharomyces cerevisiae*. Cytological and genetic analyses of these *cdc42* mutants revealed novel and diverse phenotypes, showing that Cdc42p possesses at least two distinct essential functions and acts as a nodal point of cell polarity regulation in vivo. In addition, mapping the functional data for each *cdc42* mutation onto a structural model of the protein revealed as functionally important a surface of Cdc42p that is distinct from the canonical protein-interacting domains (switch I, switch II, and the C terminus) identified previously in members of the Ras superfamily. This region overlaps with a region (α5-helix) recently predicted by structural models to be a specificity determinant for Cdc42p-protein interactions.

INTRODUCTION

Cdc42p is a member of the Rho family of the Ras superfamily of small GTP-binding proteins and is highly conserved in sequence and function across eukaryotic species (reviewed by Johnson, 1999). In mammalian cells, Cdc42p is implicated in transcriptional activation, translational control, and, via rearrangements of the actin cytoskeleton, cell morphogenesis (reviewed by Mackay and Hall, 1998; Zohn *et al.*, 1998; Johnson, 1999). In the yeast *Saccharomyces cerevisiae*, in which *CDC42* was first discovered, Cdc42p is essential for the establishment of cell polarity necessary for bud growth (Adams *et al.*, 1990; Johnson and Pringle, 1990; Johnson, 1999).

Cdc42p acts as a regulatory switch in signal transduction, cycling between an active GTP-bound state and an inactive GDP-bound state. Posttranslational C-terminal geranylgeranylation allows Cdc42p to associate with the plasma membrane, where it binds multiple downstream targets or effectors via a structural loop (switch I) (Johnson, 1999). As with other proteins in the Ras superfamily, the switch I and switch II regions of Cdc42p "switch" conformation upon replacement of bound GDP with GTP, changing the accessibility of these regions to interacting (i.e., effector) proteins (Feltham *et al.*, 1997). Although some effectors of Cdc42p thus far appear to be species specific, many Cdc42p effectors such as WASP, IQGAP, the formins, and the PAK kinases are conserved across species (Johnson, 1999). Considering the number of interactions Cdc42p makes with effector and regulatory proteins in both yeast and more complex organisms, it may be more accurate to think of Cdc42p as a signal transduction switchboard, rather than a simple "on-off" switch with one effector target. In this case, the switchboard forms multiple, distinct signaling complexes to link spatial and temporal cues within the cell to a variety of signaling pathways.

Modeling Cdc42p as a switchboard or nodal point of signal transduction, however, raises a twofold problem of specificity. First, Cdc42p must interact with specific effector targets in a temporally and spatially regulated manner. Second, to elicit specific cellular responses, molecular interactions of effector proteins with Cdc42p must be favored over interactions with other Rho family members. Specificity in these interactions could arise from a regulated spatial or temporal insulation of Cdc42p, its regulatory proteins, and/or its effectors. Alternatively, specificity may be an intrinsic property of Cdc42p. Consistent with this possibility, in vitro and in vivo studies of Rho proteins show that specific residues within switch I are required for specific cellular processes (Lamarche *et al.*, 1996; Joneson and Bar-Sagi, 1998; Sahai *et al.*, 1998; Zohar *et al.*, 1998). However, variation in switch I sequences cannot account fully for specificity. For example, in *S. cerevisiae*, there are six Rho family proteins: Cdc42p and Rho1p–Rho5p (Garcia-Ranea and Valencia, 1998). Almost all of these proteins are known to be involved in distinct functions required for budding (Cabib *et al.*, 1998; Madden and Snyder, 1998; Schmidt and Hall, 1998). The switch I regions of these proteins are highly conserved and, in the case of Cdc42p and Rho5p, identical. Therefore, it is probable that, as in the Rab family of small GTP-binding proteins (Brennwald and Novick, 1993;

* Corresponding author. E-mail address: drubin@uclink4.berkeley.edu.

Dunn *et al.*, 1993; Stenmark *et al.*, 1994), regions of Cdc42p in addition to switch I confer functional specificity. To study individual Cdc42p functions in vivo and the structure-function relationships that allow the Rho family of small GTP-binding proteins to participate in distinct cellular processes, we created and analyzed a collection of *cdc42* alleles in *S. cerevisiae*.

MATERIALS AND METHODS

Strains, Media, and Transformations

cdc42 strains generated by site-directed mutagenesis are described in Table 1. All yeast transformations were performed according to the modified (Schiestl and Gietz, 1989) method of Ito *et al.* (1983). Other strains are described below and include diploid DDY1102, which was created by mating haploid strains DDY902 (*MATa ade2-1 his3Δ200 leu2-3,112 ura3-52*) and DDY904 (MATα *his3Δ200 leu2-3,112 ura3-52 lys2-801am*).

Unless stated otherwise, yeast strains were cultured with rich (YPD) medium (Sherman *et al.*, 1986) at 25°C. To track the segregation of auxotrophic markers and to selectively maintain plasmids, strains were cultured with complete synthetic (SC) medium (Sherman *et al.*, 1986) lacking the appropriate amino acid(s) (e.g., SC-Leu). To induce sporulation, diploid cells were grown in sporulation medium (Sherman *et al.*, 1986) containing complete amino acids at one-third the concentration used for SC medium.

In Vitro Mutagenesis

To construct a *CDC42* template for mutagenesis, *S. cerevisiae CDC42* was subcloned from pRB1590 (Ohya *et al.*, 1993), on a *Bam*HI-*Sal*I fragment, into pRS305 (pDDLV29) (Sikorski and Hieter, 1989) to form pKK177. The subcloned fragment was sequenced in both directions and was found to be identical to published sequences (Johnson and Pringle, 1990; Miller and Johnson, 1997), except for a constructed *Nde*I site (CATATG) at the start codon. Site-directed mutagenesis (Transformer, Clontech, Palo Alto, CA) subsequently introduced a *Sph*I site 10 base pairs 3′ of the stop codon to generate pKK294. A *Bsu*36I-*Sph*I fragment (*Bsu*36I blunted with Klenow) was isolated from pKK294 and subcloned into the *Eco*RI (blunted with Klenow) and *Sph*I sites of pALTER-1 (Promega, Madison, WI), forming pAC2. All subsequent oligonucleotide site-directed mutagenesis was performed on pAC2 with the Altered Sites II in vitro mutagenesis system (Promega). The introduction of each mutation, marked by a diagnostic restriction site (Table 1), was verified by restriction endonuclease digestion.

From the mutagenized pAC2 template, the coding sequence of each *cdc42* allele was subcloned as a *Nde*I-*Sph*I fragment into the integration construct pKK655, replacing the *Nde*I-*Sph*I fragment bearing the wild-type allele. The D118A mutation was subcloned directly into pKK655 as a *Bsu*36I-*Bsr*GI fragment from p*cdc42-A118* (Ziman *et al.*, 1991). To construct pKK655, *LEU2* was removed from the vector sequence of pKK294 by digestion with *Tth*111I and *Dra*III, forming pKK415. *Not*I linkers were then ligated to the blunted ends of a unique *Nsi*I site in pKK415, forming pKK554. *LEU2* with *Not*I ends (underlined) was generated by PCR from a pRS305 template with the use of the primer pair 5′AGTCTCTAGCGGCCGCAC-CATATCGACTACGTCGTAAG3′ and 5′AGTCTCTAGCGGCCG-CATATCGACGGTCGAGGAG3′. This fragment was then cloned into the *Not*I site of pKK554 to form pKK655, in which the selectable *LEU2* marker is linked to *CDC42*. Integration of *LEU2* next to wild-type *CDC42* did not perceptively compromise *CDC42* function. The relevant *Ban*II-*Xba*I fragment of pKK655 is diagrammed in Figure 1C. A DNA sequence was obtained for each *cdc42* allele subcloned into pKK655 to confirm the accuracy of the mutagenesis.

Construction of cdc42 Strains

Following the strategy of Wertman *et al.* (1992), *LEU2*-marked *cdc42* alleles were integrated into the *S. cerevisiae* genome by homologous recombination (Figure 1C), replacing *CDC42* and ensuring that each *cdc42* allele was expressed at wild-type levels. A recipient strain (DDY1151) hemizygous at *CDC42* was constructed by transforming DDY1102 with a *Ban*II-*Xba*I digest of pKK366. To construct pKK366, *HIS3* was subcloned as a blunted *Apa*LI-*Dra*III fragment from pRS303 (Sikorski and Hieter, 1989) into the blunted *Nde*I sites of pKK294. Transformants of DDY1102 were selected on SC-His medium. To identify a recombinant in which one copy of the *CDC42* coding sequence was replaced by *HIS3*, His^+ transformants were screened by PCR with the use of primers A (5′CCACCGTCGAT-TCAAGGG3′) and D (5′GCTGCAAGAACAAAGAGACC3′), which flank the desired integration site (see Figure 1C). To ensure that transformation resulted in the integration of only one *HIS3* marker and did not produce any other recessive lethal mutation, hemizygotes were sporulated and the tetrad progeny dissected. For each tetrad, only two His^- progeny grew, indicating the disruption of a single essential gene by *HIS3*. The His^+ Leu^- recipient strain was then transformed with a *Ban*II-*Xba*I digest of each pKK655 derivative plasmid containing a different *cdc42* allele. Transformants were selected on SC-Leu medium. To identify homologous recombinants in which *cdc42::HIS3* was replaced by *cdc42::LEU2*, Leu^+ His^- diploids were identified by replica plating Leu^+ transformants on SC-His medium. To verify integration of a directed *cdc42* mutation linked to the *LEU2* marker at the *CDC42* locus, Leu^+ His^- diploids were screened by PCR with the use of primer A and the internal *LEU2* primer B (5′GTACCACCGAAGTCGGTGATGCTG3′) (Figure 1C). With the use of the diagnostic restriction site that marks each mutation, restriction endonuclease digestion of the PCR product confirmed the presence of each mutation at the appropriate site. To derive *cdc42* haploid strains, two or more heterozygotes from each transformation were sporulated. The progeny of 8–24 tetrads per heterozygote were dissected and scored for growth as well as for the 2:2 segregation of auxotrophic markers. As a final verification of integration, Leu^+ haploids were screened by PCR with the use of primer pairs A/B and C (5′CTTGACCAACGTGGTCACC3′)/D. As described above, restriction endonuclease digestion of the PCR product generated with primers A and B confirmed the presence of a site-directed *cdc42* mutation.

Phenotypic Analyses

In each analysis for each *cdc42* allele, at least two strains derived from independent transformants were examined. To analyze growth, *cdc42* strains were plated onto YPD or YPD supplemented with 0.9 M NaCl, 0.9 M KCl, 1.3 M sorbitol, or 3% (vol/vol) formamide (SuperPure grade; Fisher Scientific, Santa Clara, CA). In the case of recessive lethal alleles, diploids were sporulated and the tetrad progeny were dissected onto the plates described above. Plates were incubated at 25, 30, 34, and 37°C for 3 d, at 20°C for 4 d, and at 11 and 14°C for 14 d. YPG (rich medium with 3% glycerol as the sole carbon source) plates were used to test strains for impaired mitochondrial function (Sherman *et al.*, 1986).

To assess cellular morphology, log-phase cultures were examined by phase-contrast microscopy. To determine the terminal morphologies of conditional-lethal strains, log-phase cultures grown at 25°C were divided into two equal aliquots. One aliquot was maintained at 25°C and the other aliquot was shifted to a nonpermissive temperature, 14 or 37°C. At varying times during log-phase growth, aliquots were fixed in 4% formaldehyde. Before microscopic examination, each aliquot was sonicated briefly. For all morphological analyses, 200–300 cells were scored.

Peptide Antibody Production

A peptide corresponding to residues 130–145 of *S. cerevisiae* Cdc42p (see Figure 3A) was synthesized by Dr. David King (University of

Table 1. Integrated alleles of *CDC42*

Allele[a]	Mutation	Growth (YPD)[b]	Growth (YPD + 3% formamide)[c]	Restriction site[d]	DDY[e]
CDC42	None	Wild type (11–37°C)	Wild type (20–37°C)		1300
cdc42-1[f]	Multiple[h]	Conditional (11–30°C)	Conditional (25°C)	*Nla*IV (−)	1302
cdc42-101	K5A	Conditional (11–30°C)	Lethal	*Nhe*I	1304
cdc42-102	D11A	Wild type	Conditional (30°C)	*Ban*I	1306
cdc42-105	E127A,K128A	Wild type	Wild type	*Bbv*I	1308
cdc42-107	R131A,R133A,R135A	Wild type	Wild type	*Hin*dIII	1310
cdc42-108	R147A,E148A,K150A	Wild type	Wild type	*Bsr*I	1312
cdc42-109	E140A	Wild type	Wild type	*Hha*I	1314
cdc42-110	R144A	Wild type	Wild type	*Nhe*I	1316
cdc42-111	K16A	Lethal	Lethal	*Hha*I	1369
cdc42-112	D31A	Wild type	Wild type	*Bbv*I	1318
cdc42-113	D38A	Lethal	Lethal	*Nru*I	1371
cdc42-114	D48A,E49A	Wild type	Wild type	*Ban*I	1320
cdc42-115	D57A	Lethal[g]	Lethal	*Eag*I(−)	1373
cdc42-116	E62A,D63A	Conditional (20–37°C)	Lethal	*Bbv*I	1322
cdc42-117	D65A,R66A,R68A	Conditional (20–37°C)/slow	Lethal	*Pvu*I(−)	1324
cdc42-118	D76A	Conditional (11–30°C)	Conditional (25°C)	*Pst*I	1326
cdc42-119	E100A	Wild type	Conditional (20–30°C)	*Pvu*II	1328
cdc42-120	E91A,K94A,E95A,K96A	Wild type	Conditional (20–34°C)	*Pst*I	1330
cdc42-121	D170A,E171A	Wild type	Conditional (20–25°C)	*Pst*I	1332
cdc42-122	E178A	Wild type	Wild type	*Hha*I	1334
cdc42-123	R163A,K166A	Conditional (11–30°C)	Lethal	*Msc*I	1336
cdc42-124	K183A,K184A,K186A,K187A	Conditional (11–34°C)	Conditional (20–25°C)	*Bfa*I	1338
cdc42-125	K153A,E156A	Lethal	Lethal	*Bsi*WI	1383
cdc42-126	Y32K	Conditional (25°C)/slow	Lethal	*Ban*I	1340
cdc42-127	V33A	Wild type	Wild type	*Hha*I	1342
cdc42-128	T35A	Lethal	Lethal	*Pst*I	1386
cdc42-129	V36T	Conditional (20–34°C)	Lethal	*Psp*1406I	1344
cdc42-130	F37Y	Wild type	Wild type	*Acc*I	1346
cdc42-131	N39A	Wild type	Lethal	*Sfa*NI	1348
cdc42-132	Y40K	Lethal	Lethal	*Alw*NI	1390
cdc42-133	Y40C	Lethal	Lethal	*Hha*I	1391
cdc42-134	D118A	Lethal	Lethal	*Sau*3AI(−)	1392
cdc42-135	R120A,D121A,D122A,K123A	Lethal	Lethal	*Sac*II	1393
cdc42-136	R120A	Wild type	Conditional (20–34°C)	*Bgl*II	1350
cdc42-137	D121A	Wild type	Wild type	*Bsr*BI	1352
cdc42-138	D122A	Wild type	Wild type	*Sfa*NI	1354
cdc42-139	K123A	Wild type	Wild type	*Bsa*HI	1356
cdc42-140	H102A,H103A,H104A	Wild type	Conditional (20–34°C)	*Pst*I	1358

[a] Each allele, except *cdc42-1*, is linked to *LEU2*$^+$, as shown in Figure 1C.

[b] Growth phenotype of haploid cells on YPD plates at 11, 14, 20, 25, 30, 34, and 37°C. The permissive temperature range is indicated in parentheses. Relevant genotype is *cdc42*:*LEU2*$^+$ *ura3-52 leu2-3,112 his3*Δ*200 lys2-801am.*

[c] Growth phenotype of haploid cells on YPD plates containing 3% (v/v) formamide.

[d] Diagnostic restriction site added during site-directed mutagenesis to mark mutation. (−) denotes loss of the restriction site.

[e] The DDY strain number is listed for each allele of *CDC42* in a *MATa ura3-52 leu2-3,112 his3*Δ*200 lys2-801am* strain. The background of each strain is S288C. Isogenic *MAT*α haploids are designated by the next ascending odd strain number (not shown). For recessive lethal *cdc42* alleles, the listed strain number is for a diploid strain with the relevant genotype *MATa/MAT*α*, cdc42/CDC42, ade2-1/ADE2, ura3-52/ura3-52, leu2-3,112/leu2-3,112, his3*Δ*200/his3*Δ*200, lys2-801am/LYS2.*

[f] Allele isolated by Adams *et al.* (1990). Strain congenic with all other strains in this study, except *LEU2*$^+$ is at *LEU2* and unlinked to *cdc42-1.*

[g] Mutation may be dominant lethal. Only one heterozygote recovered.

[h] See Miller and Johnson (1997).

California, Berkeley). To cross-link peptide to carrier protein, 4 mg of peptide and 4 mg of rabbit serum albumin (Sigma Chemical, St. Louis, MO) were dissolved in 120 μl of 0.2 M triethanolamine-HCl, pH 8.0, in a 0.3-ml Wheaton V-vial (VWR, San Francisco, CA). Three milligrams of dimethyl-suberimidate (Sigma Chemical) were dissolved in 50 μl of the same buffer and added immediately to the peptide/carrier protein solution. The solution was stirred at room temperature for 3 h. To remove free peptide and cross-linker, the solution was dialyzed in No. 7 Spectra/Por (MWCO 1000) tubing (VWR) against 2 l of water overnight at 4°C. The dialysate was divided into aliquots and stored frozen at −20°C. The protein concentration of the dialysate was determined by the Bradford assay (Bio-Rad, Hercules, CA) with BSA as a standard.

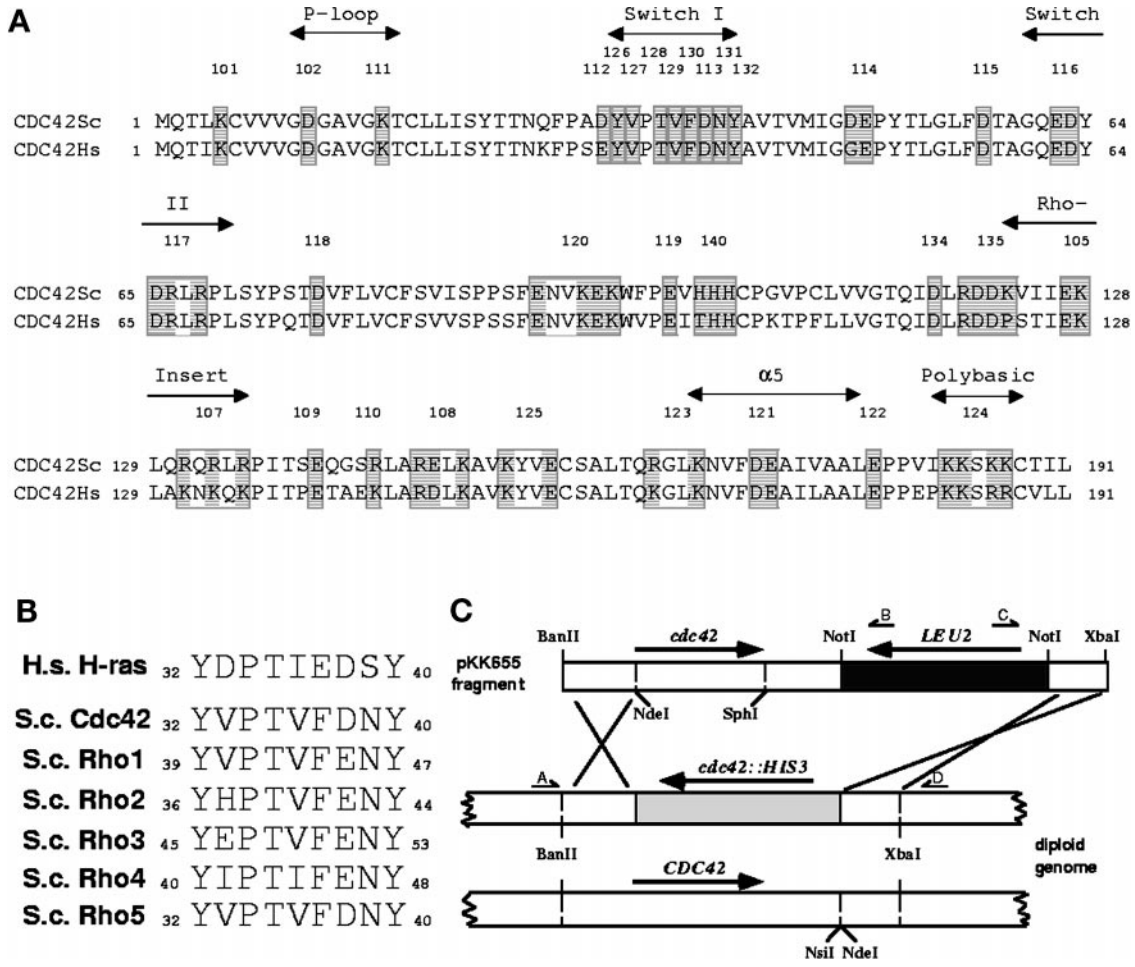

Figure 1. Cdc42p mutagenesis strategy. (A) Amino acid sequence alignment of *S. cerevisiae* Cdc42p (SwissProt P19073) and *Homo sapiens* Cdc42p (SwissProt P25763). Yeast Cdc42p residues mutagenized in this study are shaded in gray and grouped by alleles, which are designated by a number above the sequence. Alleles 133 and 136–139 are not shown but are described in Table 1. Certain secondary structure elements are demarcated by double-headed arrows. (B) Amino acid sequence alignment of the effector-binding loop or switch I domain of each Rho family protein in *S. cerevisiae*. Sequences were obtained from the *Saccharomyces* Genome Database. (C) Strategy for the genomic integration of each *LEU2*-linked *cdc42* allele into a diploid strain (His$^+$ Leu$^-$) hemizygous at the *CDC42* locus. Homologous recombination (crossed lines) between the *Ban*II-*Xba*I plasmid fragment and the chromosome containing a *HIS3* replacement of *CDC42* (*cdc42::HIS3*) results in a His$^-$ Leu$^+$ strain heterozygous at the *CDC42* locus. PCR with oligonucleotides A and D, which lie outside the region of recombination, was used in combination with oligonucleotides B and C to verify the fidelity of recombination.

New Zealand White rabbits were injected subcutaneously with 250 μg of peptide-carrier conjugate emulsified with 0.25 ml of Freund's complete adjuvant (Sigma Chemical). Booster injections containing 100 μg of conjugate mixed with Freund's incomplete adjuvant (Sigma Chemical) were administered every 3 wk after the initial injection. Bleeds were collected 2 wk after each boost, starting at wk 8, and screened for immunoreactivity against baculovirus-expressed *S. cerevisiae* GST-Cdc42p and Cdc42p in yeast whole cell lysates. Immunoreactivity against Cdc42p was first detected in the lysates at wk 17. Exsanguination occurred at wk 26.

To affinity purify the peptide antibody, a peptide column was prepared. Reacti-Gel 6X (Pierce, Rockford, IL) was washed rapidly with 0.1 M borate buffer, pH 8.8, by gentle vacuum filtration. The gel slurry was collected in a microfuge tube, and 150 μl of borate buffer containing 5 mg of peptide was added. The peptide was incubated with the gel for 48 h at room temperature with gentle rocking. To block unreacted functional groups, the gel was washed with 0.1 M Tris-Cl, pH 8.5, and incubated for 1 h at room temperature with the same buffer. Tris-Cl was then removed by sequential washes with PBS. A 1-ml column was prepared and washed successively by gravity feed with 15 ml of 6 M guanidine-HCl; 25 ml of 50 mM Tris-Cl, pH 7.4 (buffer A); 25 ml of buffer B (buffer A with 4.5 M $MgCl_2$, 1 mg/ml BSA); and 50 ml of buffer A. Fifty milliliters of serum (wk 26) pooled equally from two rabbits was cleared by centrifugation (5 min, 15,000 $\times$ *g*) and recirculated through the column for 10 h at room temperature. The column was then washed successively with 20 ml of buffer A; 40 ml of buffer A plus 1 M guanidine-Cl; and then 20 ml of buffer A. Antibody was eluted with buffer B and collected in 10 1-ml fractions. To assay for antibody in the eluate fractions, 1 μl of each fraction was diluted 1:10 in PBS and spotted onto nitrocellulose, which was then processed as a standard immunoblot. Fractions containing antibody were pooled and dialyzed against

1 l of PBS at room temperature for 3 h, followed by a second dialysis for 12 h at 4°C against 1 l of PBS containing 35% glycerol. The dialysate was divided into aliquots, frozen in N_2 (liquid), and stored at −80°C.

Microscopy

For indirect double-label immunofluorescence microscopy, cells were prepared as described by Ayscough and Drubin (1998), except the methanol/acetone permeabilization step was replaced by the addition of 6 μl of 0.05% SDS in PBS to each sample well for exactly 5 min. Affinity-purified rabbit anti-yeast Cdc42 peptide antibody and guinea pig anti-actin antibody (Mulholland *et al.*, 1994) were diluted 1:1300 and 1:2000, respectively, in PBS containing 1 mg/ml BSA. Cells were observed with epifluorescence with a Zeiss (Thornwood, NY) Axiovert microscope equipped with a 100X/1.3 Plan-Neofluar objective. Images were captured with the use of a Sony charge-coupled device camera and Northern Exposure software (Phase 3 Imaging Systems, Philadelphia, PA). For differential interference-contrast images of yeast, 0.5–1 ml of log-phase culture was briefly microfuged and resuspended in 25 μl of glucose-free minimal medium. The cells were examined immediately with a TE300 microscope (Nikon, Melville, NY) equipped with a 100X/1.4 Plan-Apo objective and a 1.4 numerical aperture condenser. Digital images were acquired with a bottom-ported Orca 100 charge-coupled device camera (Hamamatsu, Bridgewater, NJ) and Phase 3 Imaging Systems software. Image processing consisted of background subtraction and spatial filtering with a HiGauss 7 × 7 kernel convolution filter.

Intragenic Complementation Analysis

Each *cdc42*^{ts} allele in a *MATa lys2* strain (see Table 1) was mated for 6 h on YPD plates at 25°C to each *cdc42*^{ts} allele in a congenic MATα *ade2* strain (*CDC42*, DDY1601; *cdc42-1*, DDY1602; *cdc42-101*, DDY1603; *cdc42-118*, DDY1604; *cdc42-123*, DDY1605; *cdc42-124*, DDY1606; *cdc42-129*, DDY1607). Diploids were selected as single colonies on SC-Lys/Ade plates. Complementation was tested on YPD plates at 25, 30, 34, and 37°C (3 d) and scored positive if (a) a diploid that is heterozygous at the *CDC42* locus grew at temperatures that are restrictive for diploids homozygous for that *cdc42* allele present in the heterozygote; (b) a reciprocal pairwise cross yielded the same result; and (c) no reversion of the original Ts− phenotype was detected among the haploid progeny of each heterozygote.

Overexpression of Cdc42p Effectors

To determine whether overexpression of different Cdc42p effectors can suppress the growth defects of specific *cdc42*^{ts} alleles, galactose-inducible effector expression constructs were made. The coding and 3′ genomic sequences of *CLA4* (Cvrcková *et al.*, 1995) and *SKM1* (Martín *et al.*, 1997) were subcloned as *Bgl*II-*Xba*I fragments from pMJS37 and pMJS30 (both gifts of M. Shulewitz and Dr. J. Thorner, University of California, Berkeley), respectively, into the *Bam*HI and *Xba*I sites of pRB1438 (pDD42) (a gift of Dr. D. Botstein, Stanford University, Palo Alto, CA), a pRS316 (Sikorski and Hieter, 1989) vector containing a *GAL1/10* promoter (Johnston and Davis, 1984), forming p*GAL-CLA4* (pKK842) and p*GAL-SKM1* (pKK848), respectively. pCC1209 and pCC1210 are pRS316-derived plasmids in which the *GAL1/10* promoter is fused to *GIC1* and *GIC2* (Brown *et al.*, 1997; Chen *et al.*, 1997), respectively, and were the gifts of Drs. G. Chen and C. Chan (University of Texas, Austin). p*GAL-STE20* was described previously (Peter *et al.*, 1996).

The galactose-inducible overexpression plasmids were transformed into each *MATa cdc42*^{ts} strain (Table 1). To reduce background variability, each strain was grown from a single colony, prepared for transformation, and divided into individual transformation reactions. Four single colonies were picked from each SC-Ura transformation plate. A single colony derived from each independent transformant was picked and restruck to single colonies on SC-Ura plates and SC-Ura plates containing 2% galactose and 2% raffinose as the sole carbon source. The plates were first incubated at 25°C for 12 h to allow for galactose induction and then were shifted to 37°C for 6 d. Cold-sensitive strains were shifted to 14°C for 14 d, and a set of control plates was maintained at 25°C. To determine if growth at restrictive temperatures was plasmid dependent, the experiment was repeated with cells that were first grown on SC medium containing 0.5 mg/ml 5-FOA (U.S. Biological, Swampscott, MA), which counterselects *URA3*-marked plasmids (Boeke *et al.*, 1984).

Cell Extracts, SDS-PAGE, and Immunoblots

Yeast whole cell lysates were prepared as described by Belmont and Drubin (1998). A total of 0.15 OD_{600} units were loaded per lane of a 13% polyacrylamide gel prepared for SDS-PAGE (Laemmli, 1970). The gel was electrotransferred to a BA83 Protran membrane (Schleicher & Schuell, Keene, NH) for 30 min at 60 V and probed as described previously (Kozminski *et al.*, 1993), except that the Tris-buffered saline (TBS) washes included 0.1% (vol/vol) Tween 20 (Sigma Chemical). Affinity-purified rabbit anti-Cdc42 peptide antibody was diluted to 1:500 in TBS + 0.1% Tween 20 (TBST) and incubated in the same buffer for 24 h at room temperature. To block the Cdc42 peptide antibody, affinity-purified Cdc42 antibody was diluted 100-fold into 1 ml of TBS and incubated overnight at 4°C with 1 mg of the Cdc42 peptide used as an immunogen. Rabbit anti-yeast β-tubulin antibody 206 (Bond *et al.*, 1986) was diluted 1:20,000 in TBST. HRP-conjugated anti-rabbit secondary antibody (Amersham, Arlington Heights, IL) was diluted 1:5,000 in TBST and incubated for 45 min at room temperature. The blot was developed by ECL (Amersham). A dilution series of whole cell extract verified signal linearity.

Cdc42p Expression and Purification

To overexpress Cdc42p in yeast, DDY757 (*MATa cry1 ade2-1 his3-11,15 leu2-3,112 ura3-1 trp1-1 can1-100*; from A. Sachs, University of California, Berkeley) was transformed with p*GAL10-CDC42* (Miller and Johnson, 1994) to make DDY1245. To induce gene expression, log-phase cultures were washed into rich medium containing 2% (wt/vol) raffinose as the sole carbon source. Galactose was added to 2% (wt/vol) 12 h later; incubation then continued for another 8 h at 25°C before the cells were harvested.

To express Cdc42pΔC in *Escherichia coli*, the coding sequence for residues 1–183 was amplified by PCR from a pKK294 template. The fragment was subcloned into the *Nco*I (blunted with Mung Bean nuclease) and *Hin*dIII polylinker sites of pBAT4 (Peränen *et al.*, 1996), forming pKK703, and sequenced for accuracy. BL21(DE3) cells were transformed, induced, and lysed as described by Lappalainen *et al.* (1997). Because the expressed protein was insoluble, inclusion bodies were isolated from cell lysates by centrifugation at 21,000 × *g* for 30 min at 4°C. The pellet was resuspended in buffer (20 mM Tris-Cl, pH 7.5, 0.2 mM PMSF, 0.5% [vol/vol] Triton X-100), incubated on ice for 30 min, and pelleted again. Inclusion body pellets were stored at −20°C.

Baculovirus-expressed GST-Cdc42p (Zheng *et al.*, 1994) was enriched from infected *Sf*9 cells with the use of glutathione-agarose beads (Sigma Chemical), as described by Ausubel *et al.* (1994).

RESULTS

Directed Mutagenesis of CDC42 Yields a Collection of Mutants with Diverse Phenotypes

Site-directed mutagenesis of *CDC42* was used to generate mutants defective in different Cdc42p-protein interactions. One set of mutations was made in the switch I region of

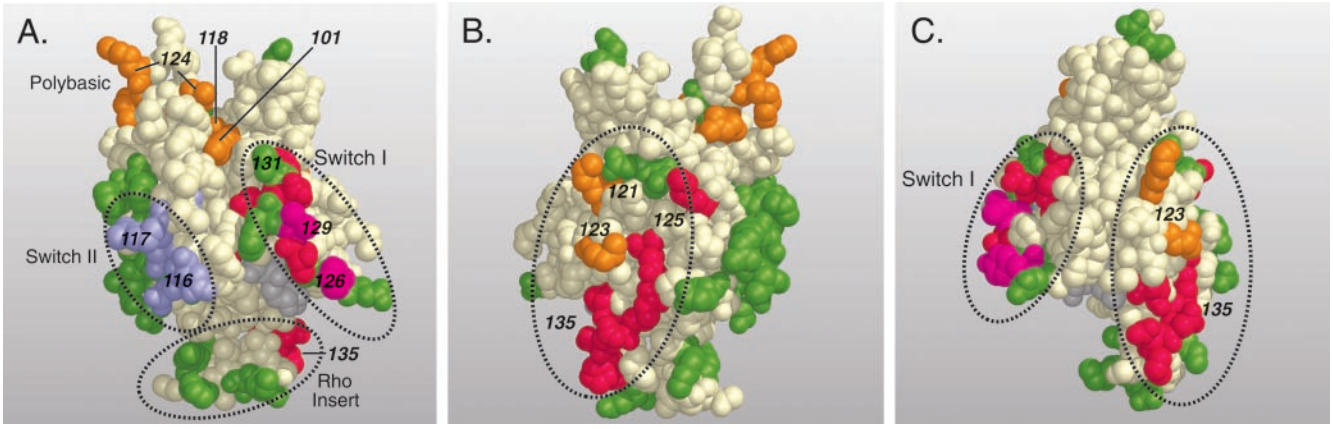

Figure 2. Space-filling model of human Cdc42p (GDP bound) shown in three different orientations (Brookhaven Protein Database accession number 1AN0). Colored residues correspond to an equivalent *S. cerevisiae* Cdc42p residue that was mutated in this study (see Figure 1A). When integrated into the *S. cerevisiae* genome, the mutations conferred lethality (red residues), temperature sensitivity (orange residues), cold sensitivity (blue residues), or both cold and temperature sensitivity (pink residues) to cells grown on rich medium. Mutations that did not confer a growth defect are colored green. GDP is colored gray. Some mutated residues are indicated by the corresponding allele number. (A) Face of Cdc42p that contains the switch I and switch II regions. (B) A 180° rotation of Cdc42p shown in A around the vertical axis. A putative intermolecular contact region is circled. (C) A left 90° rotation of Cdc42p shown in A around the vertical axis. The spatial separation of the putative intermolecular contact region shown in B from switch I is shown. The two regions are separated by a meridian of uncharged residues (uncolored).

Cdc42p (residues 32–40; Figure 1A, Table 1). Residues Y32, T35, V36, F37, and Y40 in switch I were mutated individually to amino acids that elicit a mutant phenotype when introduced into the same sequence position of Ras or Rho (Sigal *et al.*, 1986; Adari *et al.*, 1988; Calés *et al.*, 1988; Self *et al.*, 1993; Nonaka *et al.*, 1995). For switch I residues V33, D38, and N39, no previous data suggested a substitute residue. Thus, alanine replaced the target residue, removing the potentially interactive side chain. Because the switch I region is highly conserved among the six Rho proteins in *S. cerevisiae* (Figure 1B) and because no structural model existed for any Rho family member at the inception of this study, a second set of mutations was made by "alanine scanning mutagenesis" (e.g., Wertman *et al.*, 1992). Clustered charged residues have the highest probability of protein surface exposure and intermolecular contact (Chothia, 1976); therefore, in a sliding window of approximately six amino acids along the length of Cdc42p, groups of one to four charged residues were replaced with alanine (Figure 1A). In total, 37 *cdc42* alleles were created by site-directed mutagenesis.

Multiple heterozygous diploids (*cdc42/CDC42*) were recovered for each of the 37 site-directed *cdc42* alleles (Table 1), except for *cdc42-115*^{D57A}, which, consistent with a previous report (Stowers *et al.*, 1995), strongly suggests that D57A is a dominant-negative mutation. Although none of the heterozygous recombinants displayed growth defects on rich medium, two heterozygous recombinants (*cdc42-116*^{E62A,D63A}*/CDC42* and *cdc42-117*^{D65A,R66A,R68A}*/CDC42*) displayed elongate cell morphologies as a dominant phenotype.

To identify recessive growth phenotypes, the haploid progeny of each heterozygote were examined for growth on various media (Table 1). Nine of the 37 *cdc42* alleles conferred haploid lethality, and 8 alleles conferred temperature-conditional lethality on rich medium. Two of 8 temperature-conditional strains (*cdc42-117*^{D65A,R66A,R68A} and *cdc42-126*^{Y32K}) exhibited slow growth even at 25°C. *cdc42* haploid strains were also screened for sensitivity to formamide, a membrane-permeant and metabolically inert molecule known to weaken protein-protein interactions by destabilizing noncovalent bonds (Aguilera, 1994). Formamide affected the growth of 15 mutants. Eight *cdc42* alleles were found to confer formamide sensitivity at 25°C (Table 1); seven others showed enhanced temperature-sensitivity in formamide (Table 1). None of the *cdc42* alleles exhibited sensitivity to high osmolarity at 25°C. Supplementation of rich medium with 1.3 M sorbitol did suppress the growth defect of *cdc42-1*, *cdc42-101*^{K5A}, *cdc42-12*^{R163A,K166A}, *cdc42-124*^{K183A,K184A,K186A,K187A}, and *cdc42-129*^{V36T} at 37°C. 0.9 M NaCl suppressed the growth defect of only *cdc42-1*, *cdc42-101*^{K5A}, *cdc42-124*^{K183A,K184A,K186A,K187A}, and *cdc42-129*^{V36T} at 37°C. Suppression with 0.9 M KCl at 37°C was restricted to *cdc42-1* and *cdc42-101*^{K5A}. These results demonstrate that the phenotypes conferred by the site-directed *cdc42* mutations are not equivalent and that the *cdc42* mutations have different effects on cell physiology.

Relating Cdc42p Function to Structure

During the course of this study, several structural models of human Cdc42p were solved (Feltham *et al.*, 1997; Rittinger *et al.*, 1997; Nassar *et al.*, 1998). Based on the sequence identity (80%) between human and *S. cerevisiae* Cdc42p and the ability of human Cdc42p to replace *S. cerevisiae* Cdc42p in vivo (Munemitsu *et al.*, 1990; Shinjo *et al.*, 1990), we felt justified in mapping the mutations generated in this study and the functional defects associated with each onto a structural model of human Cdc42p (Figure 2). As validation of our strategy for targeting surface-exposed residues, only four mutations affected residues (K16, D57, R68, and D76) that were not fully exposed on the surface of Cdc42p. In some cases, mutations that confer the same phenotype are clustered on the surface of Cdc42p. For example, mutations

that confer only cold sensitivity (Figure 2A, blue residues) are found exclusively in the switch II region, and mutations that confer both cold and temperature sensitivity (Figure 2A, pink residues) are found exclusively in the switch I region. This clustering suggests that mutations in these regions of Cdc42p perturb a common Cdc42p function or interaction with another protein. This interpretation is supported by the cytological examination of the defects caused by these mutations (see below).

Most striking is the distribution of the lethal and conditional-lethal mutations on the surface of Cdc42p versus the mutations that did not confer a growth phenotype. Mutations that confer a growth defect can be separated into one of two distinct hemispheres on the surface of Cdc42p (Figure 2, A and B, respectively). These hemispheres are separated by a broad meridian of uncharged residues (Figure 2C) on one side and "wild-type" residues (i.e., charged residues that when mutated have no growth defect on rich medium [Figure 2B, green residues]) on the other. Growth defects resulting from mutations in the first hemisphere (Figure 2A) were expected because the guanine nucleotide-binding pocket, switch I region, and switch II region are found therein. Several mutations that confer temperature sensitivity in the presence of formamide (*cdc42-119*^{E100A}, *cdc42-120*^{E91A,K94A,E95A,K96A}, and *cdc42-140*^{H102A,H103A,H104A}) also map within this hemisphere to a region adjacent to switch II (Figure 2A, green residues behind and left of switch II). The mapping of growth defects (*cdc42-123*^{R163A,K166A}, *cdc42-125*^{K153A,E156A}, and *cdc42-135*^{R120A,D121A,D122A,K123A}; also *cdc42-121*^{D170A,E171A} in the presence of formamide) within the second hemisphere (Figure 2B) suggests the presence of an additional binding surface on Cdc42p.

This additional binding surface may be formed in part by the Rho-insert region, a 13-amino acid region (see Figure 2A and right circled region in Figure 2C) that is unique to proteins within the Rho family of the Ras superfamily (Valencia *et al.*, 1991). To determine which of the residues in the Rho-insert region are required for growth, four alleles (*cdc42-136*^{R120A}, *cdc42-137*^{D121A}, *cdc42-138*^{D122A}, and *cdc42-139*^{K123A}) were constructed with only one residue mutated per allele. None of the four alleles phenocopied the recessive lethality of *cdc42-135*^{R120A,D121A,D122A,K123A} under like conditions, indicating that no one residue within this cluster is essential for growth.

To determine whether the growth defects associated with each *CDC42* allele are attributable to aberrant Cdc42p levels, we raised a polyclonal antibody against a peptide within a region of Cdc42p (Figure 3A, boldface sequence) that is not conserved among the other five Rho proteins in *S. cerevisiae*. Immunoblots of whole cell lysates of *E. coli* expressing *S. cerevisiae* Cdc42p and wild-type yeast show that affinity-purified anti-Cdc42 peptide antibody recognizes a polypeptide of ~22 kDa, the predicted molecular mass of Cdc42p (Figure 3B). An unidentified polypeptide of ~48 kDa is also recognized by the anti-Cdc42 peptide antibody. As expected for Cdc42p, the 22-kDa polypeptide is nearly undetectable in lysates of *cdc42-1* cells, which are known to have dramatically reduced Cdc42p levels compared with wild-type strains (Ziman *et al.*, 1991). Conversely, upon galactose-induced overexpression of Cdc42p in yeast, the amount of the 22-kDa polypeptide in a yeast whole cell lysate is greater (Figure 3C, right lane) than that detected in lysates of yeast cells expressing vector alone (Figure 3C, left lane) or in uninduced cells, indicating that the peptide antibody recognizes Cdc42p in yeast whole cell lysates. Of the temperature-conditional-lethal haploid *cdc42* strains, none displayed aberrant Cdc42p levels at the permissive temperature or upon shift to a restrictive temperature (Figure 3D, top row) for a period of time known to be sufficient to elicit a terminal phenotype (Table 2 and our unpublished results). Of the non-temperature-conditional haploid strains, three alleles (*cdc42-108*^{R147A,E148A,K150A}, *cdc42-109*^{E140A}, and *cdc42-121*^{D170A,E171A}) confer reduced Cdc42p levels with respect to a wild-type control strain at 25°C (Figure 3D, bottom row). Of these three alleles, only *cdc42-109*^{E140A} contains a mutation within the Cdc42 peptide that was used as an immunogen. Therefore, the reduced Cdc42p levels conferred by *cdc42-108*^{R147A,E148A,K150A} and *cdc42-121*^{D170A,E171A} are not likely due to reduced antibody avidity. Thus far, *cdc42-108*^{R147A,E148A,K150A} is phenotypically indistinguishable from the wild type, indicating that Cdc42p is present in cells at a level beyond that required for normal vegetative growth. The lack of correlation between Cdc42p levels and the phenotypes of the mutant strains indicates that the observed phenotypes are not due to altered Cdc42p levels but result from defective Cdc42p-protein interactions.

Phenotypic Evidence for Novel cdc42 Functions

Microscopic examination of each *cdc42* haploid strain revealed even greater phenotypic diversity than was found in the initial analysis of growth. At 25°C, a temperature permissive for growth, several *cdc42* haploid strains exhibited aberrant morphologies that can be grouped into three categories: elliptical cells, cells with elongate buds, and cells of heterogenous size and shape. One hundred percent of the *cdc42-102*^{D11A} and *cdc42-116*^{E62A,D63A} haploids possessed an elliptical morphology, as opposed to the spherical morphology characteristic of wild-type haploids (Figure 4). This phenotype was more pronounced in the *cdc42-117*^{D65A,R66A,R68A} strain, in which 100% of the cells were elongate and larger than wild-type cells (Figure 4); these cells often had multiple buds and displayed a triskelion-like morphology. *cdc42-126*^{Y32K} and *cdc42-129*^{V36T} strains displayed an elongate bud morphology (Figure 4), whereas *cdc42-123*^{R163A,K166A} and *cdc42-131*^{N39A} strains exhibited a heterogenous cell size and shape. To the best of our knowledge, the morphologies of *cdc42-102*^{D11A}, *cd42-116*^{E62A,D63A}, *cdc42-117*^{D65A,R66A,R68A}, *cdc42-123*^{R163A,K166A}, and *cdc42-131*^{N39A} strains represent novel *cdc42* phenotypes and suggest the disruption of novel Cdc42p functions.

Fluorescence microscopy was used to assess the distribution of Cdc42p, the actin cytoskeleton, and the nucleus in each *cdc42* haploid strain grown in log phase at 25°C. In wild-type yeast, the anti-Cdc42 antibody recognizes an epitope at the incipient bud site and at the tips of nascent buds (Figure 5A, left), which is consistent with previously reported Cdc42p localization patterns (Ziman *et al.*, 1993). Compared with wild-type cells (Figure 5A, left), the intensity of Cdc42p staining is greatly reduced in *cdc42-1* cells (Figure 5A, right) and greatly increased in cells overexpressing Cdc42p (Figure 5B, right). Because the intensity of fluorescence in a given strain (Figure 5) correlated with the amount of Cdc42p (i.e., the 22-kDa polypeptide) in whole cell lysates of the same strain (Figure 3, B and C), we conclude that the anti-Cdc42 peptide antibody is specific for Cdc42p in cells prepared for immunofluorescence micros-

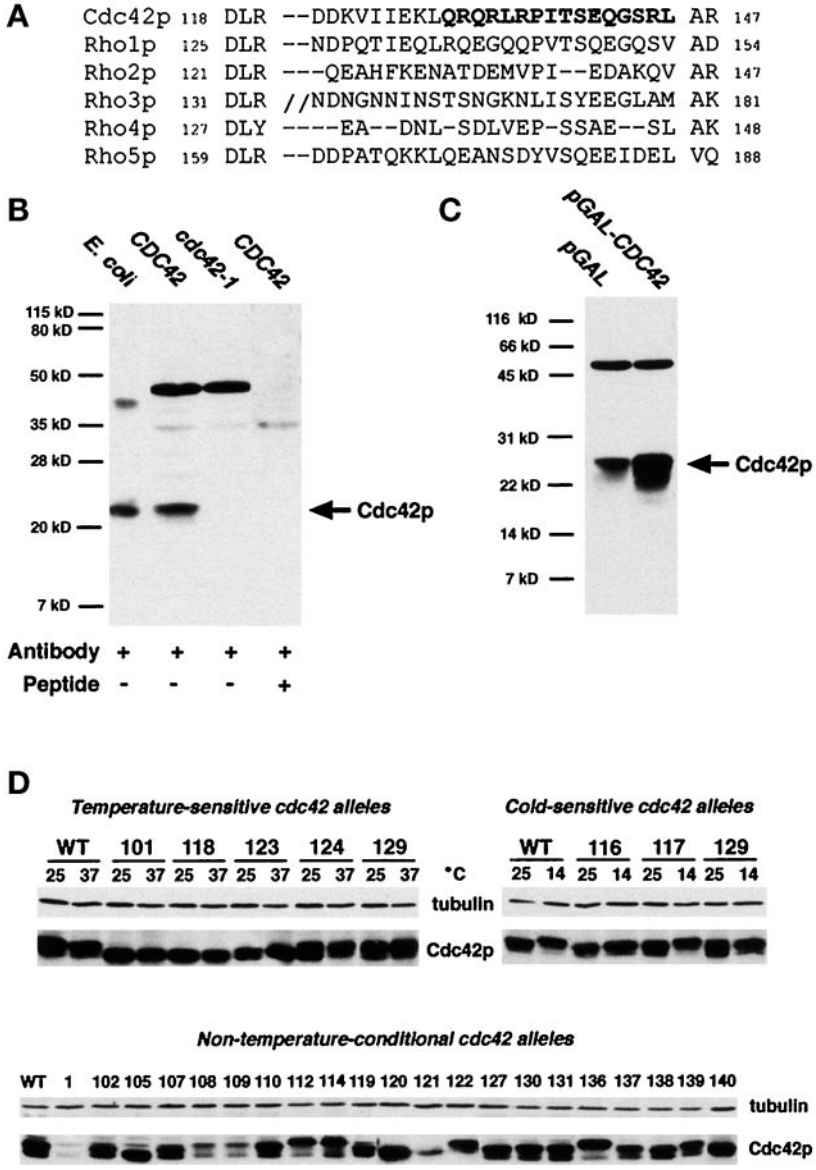

Figure 3. (A) Amino acid sequence alignment of the C-terminal variable regions of the Rho family proteins in *S. cerevisiae*. The Cdc42p peptide (residues 130–145) used as an immunogen to raise a polyclonal antibody specific for Cdc42p is shown in boldface type. (B) Immunoblot of *S. cerevisiae* Cdc42pΔC (residues 1–183) expressed in *E. coli* and whole cell lysates of wild-type (*CDC42*; DDY1300) and mutant (*cdc42-1*; DDY1302) *S. cerevisiae* probed with affinity-purified anti-Cdc42 peptide antibody or the same blocked with the peptide immunogen as indicated. (C) Immunoblots of *S. cerevisiae* whole cell lysates after galactose induction. Before harvesting, DDY1245 (carrying a GAL-CDC42 plasmid; right lane) and DDY1248 (carrying the same plasmid without the *CDC42* insert; left lane) were grown in galactose-containing medium for 8 h at 25°C. (D) Immunoblots of lysates of congenic log-phase *cdc42* haploid strains, grown in rich medium, probed with affinity-purified anti-Cdc42 peptide antibody. The same blot was probed with anti-β-tubulin to verify equivalent protein loads. An allele number is used to identify each *cdc42* strain tested. WT denotes the wild-type strain DDY1300. Temperature-sensitive *cdc42* strains were grown at 25 or 37°C for 8 h. Cold-sensitive *cdc42* strains were grown at 25 or 14°C for 18 h. Non-temperature-conditional-lethal *cdc42* strains were grown at 25°C.

copy. The same anti-Cdc42 peptide antibody revealed that Cdc42p localizes in each *cdc42* strain grown at 25°C with the same distribution described for wild-type cells, although the intensity of staining varied among the *cdc42* strains. Compared with wild-type cells, the intensity of Cdc42p staining was less in *cdc42-119*^{E100A}, *cdc42-121*^{D170A,E171A}, and *cdc42-137*^{D121A} strains and was almost undetectable in *cdc42-124*^{K183A,K184A,K186A,K187A}. Polarization of the actin cytoskeleton before budding and the fidelity of nuclear segregation were also comparable to those in wild-type cells in all but two *cdc42* strains grown at 25°C. In *cdc42-123*^{R163A,K166A} and *cdc42-129*^{V36T} cultures, the number of unbudded cells with a polarized actin cytoskeleton as a percentage of the total number of unbudded cells was 73% (n = 259) and 87% (n = 111), respectively. In contrast, in log-phase wild-type cultures or in cultures of the other temperature-sensitive strains at 25°C, only 39–48% (n = 200–259) of the total number of unbudded cells possessed a polarized actin cytoskeleton. In addition, 12 and 24% of the unbudded cells in *cdc42-123*^{R163A,K166A} and *cdc42-129*^{V36T} cultures, respectively, were multinucleate at 25°C. These results strongly suggest that *cdc42-123*^{R163A,K166A} and *cdc42-129*^{V36T} confer a unique *cdc42* phenotype, a delay in budding *after* the polarization of the actin cytoskeleton to the incipient bud site.

Microscopic examination of the *cdc42*^{ts} strains at 37°C, a temperature restrictive for growth, revealed additional phenotypic evidence for novel Cdc42p functions. After a shift from 25 to 37°C for 6 h, the *cdc42-101*^{K5A}, *cdc42-118*^{D76A}, *cdc42-123*^{R163A,K166A}, and *cdc42-124*^{K183A,K184A,K186A,K187A} strains displayed a large unbudded arrest (Figures 4 and 6, D–F), a loss of Cdc42p localization (Figure 6D; *cdc42-118*^{D76A} shown as an example), and a depolarized actin cytoskeleton

Table 2. Determination of terminal phenotypes of *cdc42*^{ts} strains at 37°C

	Hours at 37°C	Percent unbudded	Percent small budded	Percent medium budded	Percent large budded	Percent other
CDC42	0	42	30	8	19	0
	6	46	33	6	16	0
cdc42-1	0	62	30	4	5	0
	6	89	8	<1	1	2
cdc42-101	0	46	30	10	15	0
	6	97	2	1	<1	0
cdc42-118	0	56	27	2	15	0
	6	91	4	<1	4	1
cdc42-123	0	75	18	3	5	0
	6	88	4	1	2	6
cdc42-124	0	58	30	3	9	<1
	6	78	11	1	3	8
cdc42-129	0	52	23	3	3	19
	6	39	4	2	1	55

For each time point, 200 cells were scored by phase-contrast microscopy. A cell was scored as unbudded if no bud was observed, small budded if the volume of the bud appeared <30% the volume of the mother cell, medium budded if the volume of the bud appeared 30–50% the volume of the mother cell, and large budded if the volume of the bud appeared >50% the volume of the mother cell. "Other" describes grossly misshapen buds and cells, including elongate buds.

(Figure 6E), phenocopying the terminal arrest phenotype of *cdc42-1* strains (Table 2 and Adams *et al.*, 1990). At 37°C, *cdc42-101*^{K5A} and *cdc42-118*^{D76A} strains arrested as early as the first cell cycle. At 2 h after the shift to 37°C, 73 and 84% (n = 200) of the cells in *cdc42-101*^{K5A} and *cdc42-118*^{D76A} cultures, respectively, were unbudded, compared with 46% in a wild-type culture. *cdc42-129*^{V36T} cells, however, displayed a much different terminal phenotype at 37°C. At 6 h after the shift, the *cdc42-129*^{V36T} culture contained a mixed population of cells: 39% were unbudded and 55% were severely misshapen, clumped, and/or convoluted, often containing one or more elongate buds (Table 2 and Figure 4). Fluorescence microscopy of *cdc42-129*^{V36T} cells incubated at 37°C for 6 h revealed that, as at 25°C, many of the unbudded cells were multinucleate (see above); in budded cells, however, nuclear segregation appeared normal (Figure 6I). At 37°C, Cdc42p in *cdc42-129*^{V36T} cells is localized at incipient bud sites and to the bud tip (Figure 6G), along with the actin cytoskeleton (Figure 6H). This distribution of Cdc42p and actin suggests that one defect in *cdc42-129*^{V36T} cells is an inability to make a developmental switch from polarized to isotropic bud growth.

Evidence for Distinct Separable Cdc42p Functions

Phenotypic heterogeneity within the *cdc42* collection suggested that the *cdc42* alleles are defective in different functions. Identification of two *cdc42* intragenic complementation groups supports this hypothesis (Table 3). *cdc42-101*^{K5A}, *cdc42-118*^{D76A}, *cdc42-123*^{R163A,K166A}, and *cdc42-124*^{K183A,K184A,K186A,K187A} form one complementation group; these alleles failed to complement each other and therefore are defective in at least one common essential Cdc42p function. *cdc42-129*^{V36T} did complement *cdc42-101*^{K5A}, *cdc42-118*^{D76A}, *cdc42-123*^{R163A,K166A}, and *cdc42-124*^{K183A,K184A,K186A,K187A} and is the sole member of the second complementation group. *cdc42-1* did not complement any *cdc42*^{ts} allele at any temperature, suggesting that this allele has pleiotrophic effects. The two observed complementation groups correspond, respectively, to the two main morphological groups found at restrictive temperatures (large unbudded cells and cells with elongated buds), supporting the idea that the two morphological groups are due to defects in different Cdc42p-protein interactions.

Although *cdc42-101*^{K5A}, *cdc42-118*^{D76A}, *cdc42-123*^{R163A,K166A}, and *cdc42-124*^{K183A,K184A,K186A,K187A} mutants arrest as large unbudded cells at restrictive temperatures and constitute a single complementation group, these strains nevertheless differ phenotypically (e.g., differential suppression of growth defects with osmotic support; see above). Therefore, it is unlikely that these strains are solely defective in the same essential Cdc42p-dependent function. To demonstrate that these strains possess diverse *cdc42* defects, we overexpressed individually five known effectors of *S. cerevisiae* Cdc42p and tested for suppression of the temperature-sensitive growth defect at 37°C (Table 4). The growth defect conferred by *cdc42-101*^{K5A} at 37°C was suppressed by the galactose-induced overexpression of *GIC1*, a gene known to play a role in cytoskeletal polarization, but not by its close relative *GIC2* or any other Cdc42p effector tested (Brown *et al.*, 1997; Chen *et al.*, 1997). The growth defect conferred by *cdc42-118*^{D76A} at 37°C was suppressed by the overexpression of *STE20*, a serine/threonine kinase of the PAK family (Peter *et al.*, 1996; Leberer *et al.*, 1997) known to be involved in cytoskeletal regulation (Eby *et al.*, 1998). Overexpression of *STE20* only weakly suppressed the growth defects of *cdc42-1* and *cdc42-123*^{R163A,K166A}. *cdc42-129*^{V36T}, which is in a different intragenic complementation group from *cdc42-101*^{K5A}, *cdc42-118*^{D76A}, and *cdc42-123*^{R163A,K166A}, was only weakly suppressed at 37°C by the overexpression of the PAK family kinases *CLA4* (Cvrcková *et al.*, 1995) and *SKM1* (Martín *et al.*, 1997), although *CLA4* overexpression can suppress the

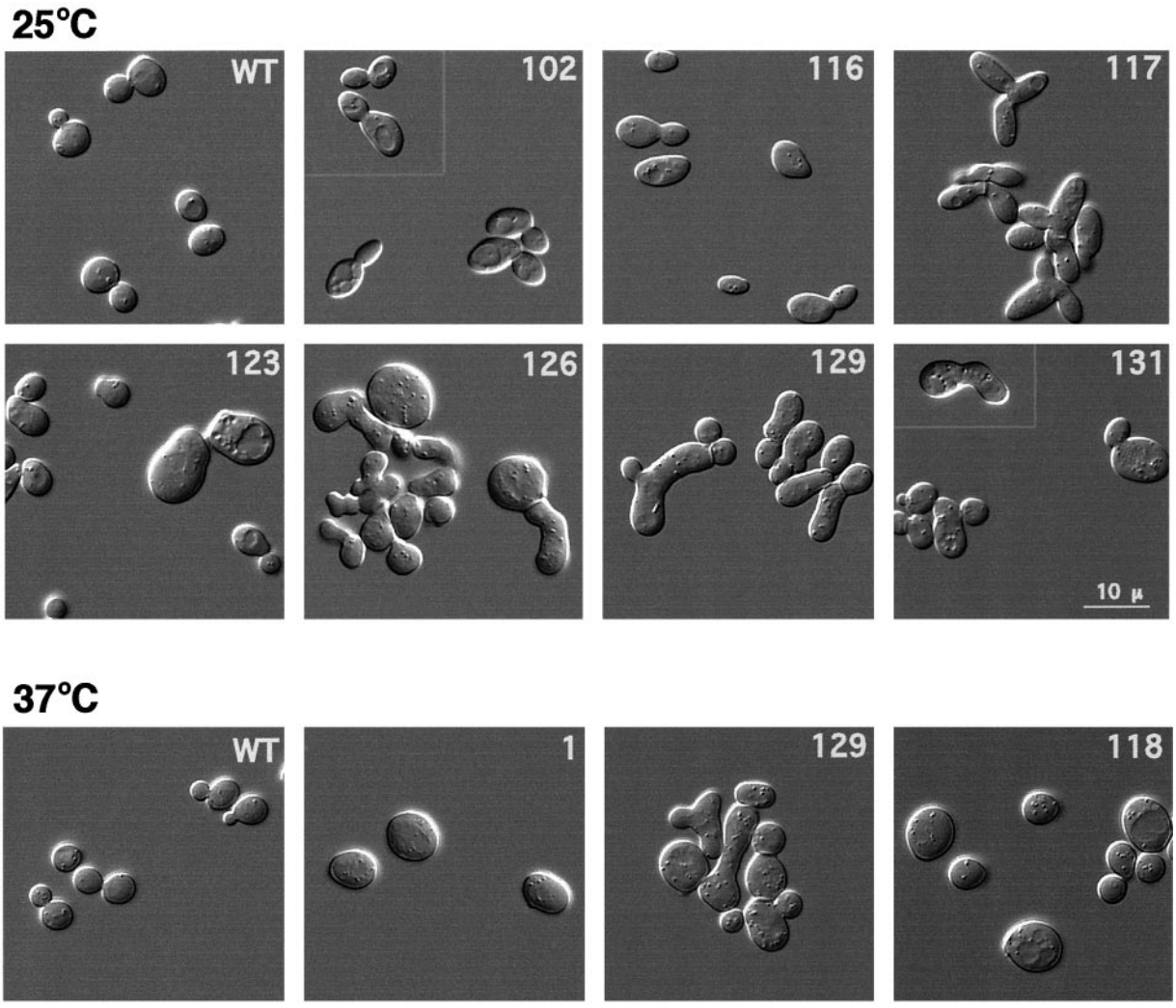

Figure 4. Differential interference-contrast images of haploid *cdc42* mutants (labeled with *cdc42* allele number) in log phase in rich medium at 25 or 37°C (5–6 h after the shift from 25°C).

cold sensitivity of *cdc42-129*^{V36T} at 14°C. These results indicate that the *cdc42*^{ts} alleles perturb distinct Cdc42p functions and provide evidence that these Cdc42p functions can be attributed to distinct surfaces and protein–Cdc42p interactions.

DISCUSSION

Separation-of-function alleles are required to enumerate the Cdc42-dependent steps in morphogenesis/cell division and to determine whether one or more Cdc42p-protein interactions are required for each step. Four lines of evidence presented in this study reveal novel roles for Cdc42p and show that bud formation involves multiple essential Cdc42p interactions. First, *cdc42* mutants show a diversity of morphological defects. Second, *cdc42*^{ts} mutants fall into two intragenic complementation groups. Third, genes encoding Cdc42p effectors confer allele-specific dosage suppression of *cdc42* conditional-lethal mutants. Fourth, four *cdc42* mutants that arrest as large unbudded cells under restrictive conditions show differential suppression of growth defects on different media.

The elongate buds observed in one *cdc42* complementation group (i.e., *cdc42-129*^{V36T}) suggest that one distinct function of Cdc42p is to facilitate the developmental switch from polarized to isotropic bud growth during G2 of the cell cycle. During this switch, the cortical actin cytoskeleton, which is localized to regions of active cell growth (Adams and Pringle, 1984), must be redistributed from the bud tip to the circumference of the bud. Because overexpression of constitutively active Cdc42p (G12V or Q61L) is known to result in elongate buds (Ziman *et al.*, 1991), it is possible that Cdc42p is not properly down-regulated in *cdc42-129*^{V36T} cells during G2. The recessive nature of *cdc42-129*^{V36T}, however, suggests a loss rather than a gain of Cdc42p function; i.e., *cdc42-129*^{V36T} cells may have lost the ability to generate

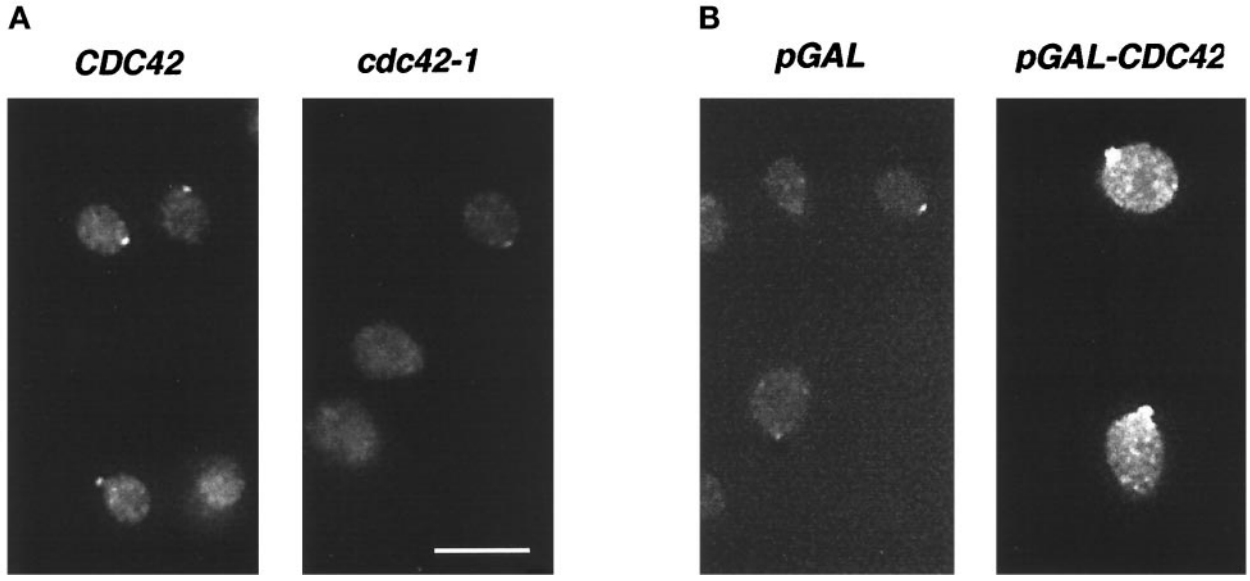

Figure 5. (A) Indirect immunofluorescence of wild-type (*CDC42*; DDY1300) and mutant (*cdc42-1*; DDY1302) *S. cerevisiae* grown at 25°C in rich medium and probed with affinity-purified anti-Cdc42 peptide antibody. Bar, 10 μm. (B) Indirect immunofluorescence of *S. cerevisiae* cells, from the same cultures described in Figure 3C, probed with affinity-purified anti-Cdc42 peptide antibody. The scale is the same as in A.

a signal that promotes the redistribution of the actin cytoskeleton in G2. The Cdc42p-dependent activation of the kinase Gin4p via the Cdc42p effector Cla4p is required for the switch from apical to isotropic bud growth (Tjandra *et al.*, 1998). Several lines of evidence suggest that the hyperpolarized bud growth observed in *cdc42-129*^{V36T} cells is due to a defect in this pathway. First, defects in Cla4p and Gin4p function phenocopy the morphology of *cdc42-129*^{V36T} cells. Specifically, *gin4*Δ in a Clb2p-dependent background (Altman and Kellogg, 1997), *cla4*Δ, and *cla4*^{ts} (Cvrcková *et al.*, 1995; Tjandra *et al.*, 1998; Weiss and Drubin, unpublished results) all confer elongate buds. Second, the growth defect associated with *cdc42-129*^{V36T} at 14°C is specifically suppressed by the overexpression of *CLA4*. Third, Gin4p kinase activity is reduced in *cdc42-129*^{V36T} cells (Tjandra and Kellogg, personal communication). Thus, the product encoded by *cdc42-129*^{V36T} is predicted to be defective in its interaction with Cla4p.

Mutations in the switch II region of Cdc42p also confer a defect in morphogenesis; however, in contrast to the recessive *cdc42-129*^{V36T} allele, *cdc42-116*^{E62A,D63A} and *cdc42-117*^{D65A,R66A,R68A} are dominant for their morphological phenotypes. Recent modeling of a human Cdc42p-GTPase–activating protein (GAP) complex indicates that E62 and D63 of the Cdc42p switch II region are in contact with a GAP (Rittinger *et al.*, 1997; Nassar *et al.*, 1998). In *S. cerevisiae*, failure to properly interact with one or more of the Cdc42-GAPs (i.e., Bem3p, Rga1p, and Rga2p) may be the cause of the elongate morphology and cold sensitivity conferred by *cdc42-116*^{E62A,D63A} and *cdc42-117*^{D65A,R66A,R68A}. Similar morphologies are observed in *S. cerevisiae* when the known Cdc42-GAPs suffer a concomitant loss of function (Smith and Sprague, personal communication), strongly supporting the idea that *cdc42-116*^{E62A,D63A} and *cdc42-117*^{D65A,R66A,R68A} are defective in GAP binding.

The structural model of the human Cdc42p-GAP complex also shows an intramolecular hydrogen bond between D76, which is just C terminal to switch II, and R187 (K in *S. cerevisiae*), which is in the C-terminal polybasic region of Cdc42p (Nassar *et al.*, 1998). This interaction is predicted to stabilize the C terminus of Cdc42p for its interaction with the GAP. Consistent with this model, both *cdc42-118*^{D76A} and *cdc42-124*^{K183A,K184A,K186A,K187A} share the same terminal phenotype, which is the expected result if both mutations cause a defect in the same interaction. However, the phenotype of large, unbudded, multinucleate cells with a depolarized actin cytoskeleton at 37°C is itself inconsistent with impaired GAP-stimulated GTP hydrolysis, which would be expected to confer a more highly polarized (elongate) morphology, as observed with *cdc42-116*^{E62A,D63A} and *cdc42-117*^{D65A,R66A,R68A} cells (see above) or with cells overexpressing constitutively active *CDC42* (Ziman *et al.*, 1991; Davis *et al.*, 1998). Therefore, if D76 does indeed stabilize the C terminus in vivo, it may be to promote the interaction of the C terminus with proteins that down-regulate Cdc42p activity (e.g., GDI) and/or effectors of Cdc42p (e.g., Ste20p).

The Rho-insert region may also stabilize intermolecular contacts. Structural (Feltham *et al.*, 1997) and biochemical (McCallum *et al.*, 1996) studies suggest that the Rho-insert region of Cdc42p (residues 122–134) is a secondary binding site or "footrest" for effectors that bind to switch I. The Rho-insert region clearly has a role because deletion of this region abolishes the transforming activity of a mutant human Cdc42p (F28L) (Wu *et al.*, 1998). As demonstrated with Rac (Joseph and Pick, 1995; Freeman *et al.*, 1996; Wei *et al.*, 1997), this region may be important for target specificity. Even though one allele (*cdc42-135*^{R120A,D121A,D122A,K123A}) consisting of mutations within the insert region resulted in a growth defect, supporting recent observations that this region of Cdc42p is functionally important, no other mutations

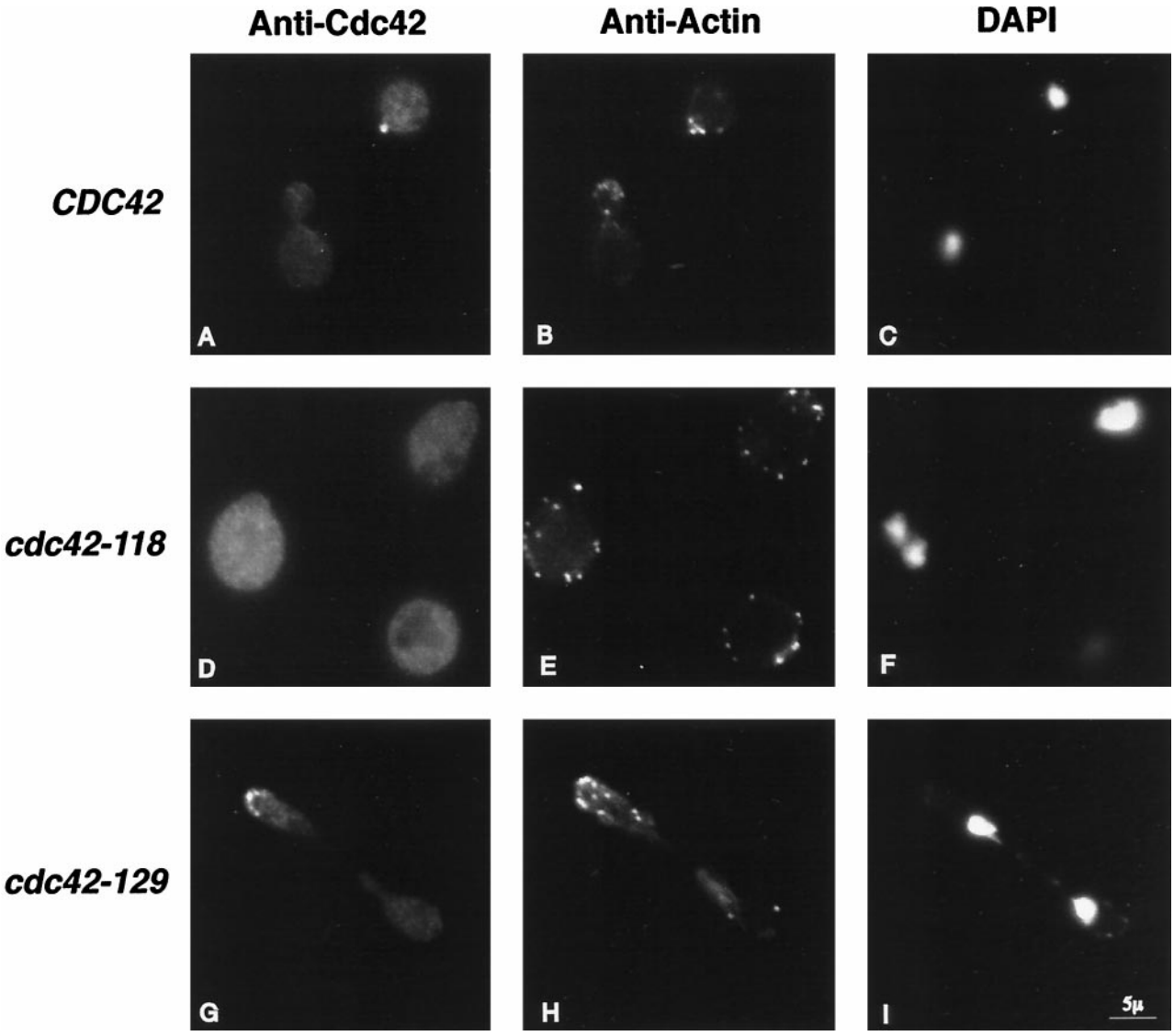

Figure 6. Fluorescence images of wild-type (*CDC42*; DDY1300; top row), *cdc42-118*^{D76A} (DDY1326), and *cdc42-129*^{V36T} (DDY1344) cells shifted from 25 to 37°C for 6 h and probed with affinity-purified Cdc42 peptide antibody (left column), affinity-purified anti-actin antibody (middle column), or DAPI for DNA (right column).

(i.e., *cdc42-105*^{E127A,K128A} and *cdc42-107*^{R131A,R133A,R135A}) yielded a functional defect. This observation suggests that only part of the Rho-insert region in Cdc42p is important for functional interactions.

Overlapping the Rho-insert region on the face of Cdc42p opposite switch I and switch II, a putative binding region (Figure 2B) is defined by *cdc42-135*^{R120A,D121A,D122A,K123A} and by the conditional-lethal alleles *cdc42-121*^{D170A,E171A} and *cdc42-123*^{R163A,K166A}. Although the residues mutated in the recessive-lethal allele *cdc42-125*^{K153A,E156A} are located in this region as well, these residues are part of a conserved GTP-binding/hydrolysis domain. Therefore, the lethality associated with *cdc42-125*^{K153A,E156A}, as well as that of *cdc42-111*^{K16A}, *cdc42-115*^{D57A}, and *cdc42-134*^{D118A}, is more likely to be the result of defective nucleotide binding/hydrolysis than defective Cdc42p-protein interactions. The residues mutated in both *cdc42-121*^{D170A,E171A} and *cdc42-123*^{R163A,K166A} are part of the C-terminal α5-helix. In support of our functional mapping data, which suggest that this region forms an additional intermolecular contact site and contributes to the specificity of Cdc42p interactions in vivo, recent nuclear magnetic resonance data show contact between the α5-helix of human Cdc42p and the CRIB (Cdc42/Rac interactive binding) motif–containing GTPase-binding domains of WASP (Abdul-Manan *et al.*, 1999), PAK (Guo *et al.*, 1998; Stevens *et al.*, 1999), and ACK tyrosine kinase (Mott *et al.*, 1999). These structural data suggest that the α5-helix of Cdc42p is a specificity determinant (Guo *et al.*, 1998; Abdul-Manan *et al.*, 1999; Mott *et al.*, 1999). Consistent with our in vivo data demonstrating a loss of function when K166 is

Table 3. Intragenic complementation analysis of *cdc42*^{ts} alleles

	CDC42	*cdc42-101*	*cdc42-118*	*cdc42-123*	*cdc42-124*	*cdc42-129*	*cdc42-1*
CDC42	+						
cdc42-101	+	−					
cdc42-118	+	−	−				
cdc42-123	+	−	−	−			
cdc42-124	+	−	−	−	−		
cdc42-129	+	+	+	+	+	−	
cdc42-1	+	−	−	−	−	−	−

Pairwise crosses between each *cdc42*^{ts} allele were made by mating each haploid *cdc42*^{ts} strain to each other. The diploid cells resulting from the mating were struck to single colonies on rich medium and scored for growth after incubation at 34°C for 2 d. + indicates wild type growth, − indicates no growth (no single colonies). Reciprocal pairwise crosses in which the mating type of the strain containing each allele was reversed yielded identical results (not shown).

Table 4. Suppression of *cdc42*^{ts} growth defect by effector overexpression

	Vector	*STE20*	*CLA4*	*SKM1*	*GIC1*	*GIC2*
CDC42	+	+	−	+	+	+
cdc42-101	−	−	−	−	+	−
cdc42-118	−	+	−	−	−	−
cdc42-123	−	+/−	−	−	+/−	+/−
cdc42-129	−	−	+/−	+/−	−	−
cdc42-1	−	+/−	−	−	+/−	−

cdc42^{ts} strains (*MATa*; see Table 1) were transformed with galactose-inducible *URA3*-marked *cen* plasmids containing known effectors of Cdc42. Transformation with vector (pRB1438), p*GAL-STE20*, p*GAL-CLA4*, p*GAL-SKM1*, p*GAL-GIC1*, and p*GAL-GIC2* yielded, respectively, *CDC42*: DDY 1610, 1611, 1612, 1613, 1614, 1615; *cdc42-1*: DDY 1616, 1617, 1618, 1619, 1620, 1621; *cdc42-101*: DDY 1622, 1623, 1624, 1625, 1626, 1627; *cdc42-118*: DDY 1628, 1629, 1630, 1631, 1632, 1633; *cdc42-123*: DDY 1634, 1635, 1636, 1637, 1638, 1639; and *cdc42-129*: DDY 1640, 1641, 1642, 1643, 1644, 1645. Transformants were struck to single colonies on selective medium containing galactose and incubated at 37°C. + indicates wild type growth, +/− indicates weak growth, and − indicates no growth (single colonies). Overexpression of *CLA4* inhibits the growth of wild-type cells at 37°C but not 25°C. *cdc42-124* was not included in this analysis because it is not temperature sensitive on selective media.

mutated to alanine, the Cdc42p-ACK solution structure shows P513 of ACK tyrosine kinase packed against K166 of human Cdc42p (Mott *et al.*, 1999). Of particular relevance to *cdc42-121*^{D170A,E171A}, the Cdc42p-WASP solution structure shows hydrogen bonding between E171 of Cdc42p and K235 of WASP (Abdul-Manan *et al.*, 1999). Although it is tempting to speculate that the growth defect conferred by *cdc42-121*^{D170A,E171A} is due to a defective Cdc42p interaction with the yeast homologue of WASP, Las17p, no CRIB motif exists in Las17p (Burbelo *et al.*, 1995), making a similar binding interaction unlikely. Therefore, in *S. cerevisiae* at least, the Cdc42p α5-helix may serve as a site of intermolecular contact and as a specificity determinant for Cdc42p effectors, other than Las17p, that contain a CRIB motif.

The extensiveness of our analyses in vivo and the recent availability of Cdc42p structural models (Feltham *et al.*, 1997; Rittinger *et al.*, 1997; Nassar *et al.*, 1998) have provided an opportunity to relate Cdc42p function to structure. Although studies of Ras established a paradigm for relating the structure of a small GTP-binding protein to function (Bourne *et al.*, 1991; Valencia *et al.*, 1991; Zerial and Huber, 1995; Campbell *et al.*, 1998), distinct differences have been shown between the structure-function relationships of Ras and Rho proteins (Valencia *et al.*, 1991; Ziman *et al.*, 1991; Self *et al.*, 1993; Xu *et al.*, 1994; Joseph and Pick, 1995; Li and Zheng, 1997; Hoffman *et al.*, 1998). Therefore, Ras models cannot define all of the structure-function relationships of Cdc42p. In addition to identifying novel functions and functional domains of Cdc42p, our results have formed a broad genetic foundation for the continuing analysis of a highly conserved signal transduction molecule.

ACKNOWLEDGMENTS

The authors thank K. Ayscough, G. Barnes, B. Bart, L. Belmont, I. Cheeseman, M. Duncan, B. Goode, C. Hofmann, P. Lappalainen, and E. Weiss for critical advice and comments. We also thank D. King for very helpful advice on peptide chemistry and J. Cope for patient assistance with the structural graphics. We thank D. Botstein, C. Chan, G. Chen, D. Kellogg, M. Molina, M. Peter, M. Shulewitz, F. Solomon, J. Thorner, and Y. Zheng for kindly supplying reagents. This work was supported by a Helen Hay Whitney Postdoctoral Fellowship to K.G.K., a Howard Hughes Medical Institute Predoctoral Fellowship to A.A.R., and National Institutes of Health grant GM50399 to D.G.D.

REFERENCES

Abdul-Manan, N., Aghazadeh, B., Liu, G.A., Majumdar, A., Ouerfelli, O., Siminovitch, K.A., and Rosen, M.K. (1999). Structure of Cdc42 in complex with the GTPase-binding domain of the 'Wiskott-Aldrich syndrome' protein. Nature *399*, 379–383.

Adams, A.E., Johnson, D.I., Longnecker, R.M., Sloat, B.F., and Pringle, J.R. (1990). *CDC42* and *CDC43*, two additional genes involved in budding and the establishment of cell polarity in the yeast *Saccharomyces cerevisiae*. J. Cell Biol. *111*, 131–142.

Adams, A.E., and Pringle, J.R. (1984). Relationship of actin and tubulin distribution to bud growth in wild-type and morphogenetic-mutant *Saccharomyces cerevisiae*. J. Cell Biol. *98*, 934–945.

Adari, H., Lowy, D.R., Willumsen, B.M., Der, C.J., and McCormick, F. (1988). Guanosine triphosphatase activating protein (GAP) interacts with the p21 *ras* effector binding domain. Science *240*, 518–521.

Aguilera, A. (1994). Formamide sensitivity: a novel conditional phenotype in yeast. Genetics *136*, 87–91.

Altman, R., and Kellogg, D. (1997). Control of mitotic events by Nap1 and the Gin4 kinase. J. Cell Biol. *138*, 119–130.

Ausubel, F.M., Brent, R., Kingston, R.E., Moore, D.D., Seidman, J.G., Smith, J.A., and Struhl, K. (1994). Current Protocols in Molecular Biology, New York: John Wiley & Sons.

Ayscough, K.R., and Drubin, D.G. (1998). Immunofluorescence microscopy of yeast cells. In: Cell Biology: A Laboratory Handbook, vol. 2, ed. J. Celis, New York: Academic Press, 447–485.

Belmont, L.D., and Drubin, D.G. (1998). The yeast V159N actin mutant reveals roles for actin dynamics in vivo. J. Cell Biol. *142*, 1289–1299.

Boeke, J.D., LaCroute, F., and Fink, G.R. (1984). A positive selection for mutants lacking orotidine-5′-phosphate decarboxylase activity in yeast: 5-fluoro-orotic acid resistance. Mol. Gen. Genet. *197*, 345–346.

Bond, J.F., Fridovich-Keil, J.L., Pillus, L., Mulligan, R.C., and Solomon, F. (1986). A chicken-yeast chimeric β-tubulin protein is incorporated into mouse microtubules in vivo. Cell *44*, 461–468.

Bourne, H.R., Sanders, D.A., and McCormick, F. (1991). The GTPase superfamily: conserved structure and molecular mechanism. Nature *349*, 117–127.

Brennwald, P., and Novick, P. (1993). Interactions of three domains distinguishing the Ras-related GTP-binding proteins Ypt1 and Sec4. Nature *362*, 560–563.

Brown, J.L., Jaquenoud, M., Gulli, M.P., Chant, J., and Peter, M. (1997). Novel Cdc42-binding proteins Gic1 and Gic2 control cell polarity in yeast. Genes Dev. *11*, 2972–2982.

Burbelo, P.D., Drechsel, D., and Hall, A. (1995). A conserved binding motif defines numerous candidate target proteins for both Cdc42 and Rac GTPases. J. Biol. Chem. *270*, 29071–29074.

Cabib, E., Drgonová, J., and Drgon, T. (1998). Role of small G proteins in yeast cell polarization and wall biosynthesis. Annu. Rev. Biochem. *67*, 307–333.

Calés, C., Hancock, J.F., Marshall, C.J., and Hall, A. (1988). The cytoplasmic protein GAP is implicated as the target for regulation by the *ras* gene product. Nature *332*, 548–551.

Campbell, S.L., Khosravi-Far, R., Rossman, K.L., Clark, G.J., and Der, C.J. (1998). Increasing complexity of Ras signaling. Oncogene *17*, 1395–1413.

Chen, G.C., Kim, Y.J., and Chan, C.S. (1997). The Cdc42 GTPase-associated proteins Gic1 and Gic2 are required for polarized cell growth in *Saccharomyces cerevisiae*. Genes Dev. *11*, 2958–2971.

Chothia, C. (1976). The nature of the accessible and buried surfaces in proteins. J. Mol. Biol. *105*, 1–12.

Cvrcková, F., De Virgilio, C., Manser, E., Pringle, J.R., and Nasmyth, K. (1995). Ste20-like protein kinases are required for normal localization of cell growth and for cytokinesis in budding yeast. Genes Dev. *9*, 1817–1830.

Davis, C.R., Richman, T.J., Deliduka, S.B., Blaisdell, J.O., Collins, C.C., and Johnson, D.I. (1998). Analysis of the mechanisms of action of the *Saccharomyces cerevisiae* dominant lethal *cdc42G12V* and dominant negative *cdc42D118A* mutations. J. Biol. Chem. *273*, 849–858.

Dunn, B., Stearns, T., and Botstein, D. (1993). Specificity domains distinguish the Ras-related GTPases Ypt1 and Sec4. Nature *362*, 563–565.

Eby, J.J., Holly, S.P., van Drogen, F., Grishin, A.V., Peter, M., Drubin, D.G., and Blumer, K.J. (1998). Actin cytoskeleton organization regulated by the PAK family of protein kinases. Curr. Biol. *8*, 967–970.

Feltham, J.L., Dötsch, V., Raza, S., Manor, D., Cerione, R.A., Sutcliffe, M.J., Wagner, G., and Oswald, R.E. (1997). Definition of the switch surface in the solution structure of Cdc42Hs. Biochemistry *36*, 8755–8766.

Freeman, J.L., Abo, A., and Lambeth, J.D. (1996). Rac "insert region" is a novel effector region that is implicated in the activation of NADPH oxidase, but not PAK65. J. Biol. Chem. *271*, 19794–19801.

Garcia-Ranea, J.A., and Valencia, A. (1998). Distribution and functional diversification of the ras superfamily in *Saccharomyces cerevisiae*. FEBS Lett. *434*, 219–225.

Guo, W., Sutcliffe, M.J., Cerione, R.A., and Oswald, R.E. (1998). Identification of the binding surface on Cdc42Hs for p21-activated kinase. Biochemistry *37*, 14030–14037.

Hoffman, G.R., Nassar, N., Oswald, R.E., and Cerione, R.A. (1998). Fluoride activation of the Rho family GTP-binding protein Cdc42Hs. J. Biol. Chem. *273*, 4392–4399.

Ito, H., Fukuda, Y., Murata, K., and Kimura, A. (1983). Transformation of intact yeast cells treated with alkali cations. J. Bacteriol. *153*, 163–168.

Johnson, D.I. (1999). Cdc42: an essential Rho-type GTPase controlling eukaryotic cell polarity. Microbiol. Mol. Biol. Rev. *63*, 54–105.

Johnson, D.I., and Pringle, J.R. (1990). Molecular characterization of *CDC42*, a *Saccharomyces cerevisiae* gene involved in the development of cell polarity. J. Cell Biol. *111*, 143–152.

Johnston, M., and Davis, R.W. (1984). Sequences that regulate the divergent *GAL1-GAL10* promoter in *Saccharomyces cerevisiae*. Mol. Cell. Biol. *4*, 1440–1448.

Joneson, T., and Bar-Sagi, D. (1998). A Rac1 effector site controlling mitogenesis through superoxide production. J. Biol. Chem. *273*, 17991–17994.

Joseph, G., and Pick, E. (1995). "Peptide walking" is a novel method for mapping functional domains in proteins: its application to the Rac1-dependent activation of NADPH oxidase. J. Biol. Chem. *270*, 29079–29082.

Kozminski, K.G., Diener, D.R., and Rosenbaum, J.L. (1993). High level expression of nonacetylatable α-tubulin in *Chlamydomonas reinhardtii*. Cell Motil. Cytoskeleton *25*, 158–170.

Laemmli, U.K. (1970). Cleavage of structural proteins during the assembly of the head of bacteriophage T4. Nature *227*, 680–685.

Lamarche, N., Tapon, N., Stowers, L., Burbelo, P.D., Aspenström, P., Bridges, T., Chant, J., and Hall, A. (1996). Rac and Cdc42 induce actin polymerization and G1 cell cycle progression inde-

pendently of p65^{PAK} and the JNK/SAPK MAP kinase cascade. Cell *87*, 519–529.

Lappalainen, P., Fedorov, E.V., Fedorov, A.A., Almo, S.C., and Drubin, D.G. (1997). Essential functions and actin-binding surfaces of yeast cofilin revealed by systematic mutagenesis. EMBO J. *16*, 5520–5530.

Leberer, E., Wu, C., Leeuw, T., Fourest-Lieuvin, A., Segall, J.E., and Thomas, D.Y. (1997). Functional characterization of the Cdc42p binding domain of yeast Ste20p protein kinase. EMBO J. *16*, 83–97.

Li, R., and Zheng, Y. (1997). Residues of the Rho family GTPases Rho and Cdc42 that specify sensitivity to Dbl-like guanine nucleotide exchange factors. J. Biol. Chem. *272*, 4671–4679.

Mackay, D.J., and Hall, A. (1998). Rho GTPases. J. Biol. Chem. *273*, 20685–20688.

Madden, K., and Snyder, M. (1998). Cell polarity and morphogenesis in budding yeast. Annu. Rev. Microbiol. *52*, 687–744.

Martín, H., Mendoza, A., Rodríguez-Pachón, J.M., Molina, M., and Nombela, C. (1997). Characterization of *SKM1*, a *Saccharomyces cerevisiae* gene encoding a novel Ste20/PAK-like protein kinase. Mol. Microbiol. *23*, 431–444.

McCallum, S.J., Wu, W.J., and Cerione, R.A. (1996). Identification of a putative effector for Cdc42Hs with high sequence similarity to the RasGAP-related protein IQGAP1 and a Cdc42Hs binding partner with similarity to IQGAP2. J. Biol. Chem. *271*, 21732–21737.

Miller, P.J., and Johnson, D.I. (1994). Cdc42p GTPase is involved in controlling polarized cell growth in *Schizosaccharomyces pombe*. Mol. Cell. Biol. *14*, 1075–1083.

Miller, P.J., and Johnson, D.I. (1997). Characterization of the *Saccharomyces cerevisiae cdc42-1*^{ts} allele and new temperature-conditional-lethal cdc42 alleles. Yeast *13*, 561–572.

Mott, H.R., Owen, D., Nietlispach, D., Lowe, P.N., Manser, E., Lim, L., and Laue, E.D. (1999). Structure of the small G protein Cdc42 bound to the GTPase-binding domain of ACK. Nature *399*, 384–388.

Mulholland, J., Preuss, D., Moon, A., Wong, A., Drubin, D., and Botstein, D. (1994). Ultrastructure of the yeast actin cytoskeleton and its association with the plasma membrane. J. Cell Biol. *125*, 381–391.

Munemitsu, S., Innis, M.A., Clark, R., McCormick, F., Ullrich, A., and Polakis, P. (1990). Molecular cloning and expression of a G25K cDNA, the human homolog of the yeast cell cycle gene CDC42. Mol. Cell. Biol. *10*, 5977–5982.

Nassar, N., Hoffman, G.R., Manor, D., Clardy, J.C., and Cerione, R.A. (1998). Structures of Cdc42 bound to the active and catalytically compromised forms of Cdc42GAP. Nat. Struct. Biol. *5*, 1047–1052.

Nonaka, H., Tanaka, K., Hirano, H., Fujiwara, T., Kohno, H., Umikawa, M., Mino, A., and Takai, Y. (1995). A downstream target of *RHO1* small GTP-binding protein is *PKC1*, a homolog of protein kinase C, which leads to activation of the MAP kinase cascade in *Saccharomyces cerevisiae*. EMBO J. *14*, 5931–5938.

Ohya, Y., Qadota, H., Anraku, Y., Pringle, J.R., and Botstein, D. (1993). Suppression of yeast geranylgeranyl transferase I defect by alternative prenylation of two target GTPases, Rho1p and Cdc42p. Mol. Biol. Cell *4*, 1017–1025.

Peränen, J., Rikkonen, M., Hyvönen, M., and Kääriäinen, L. (1996). T7 vectors with modified T7*lac* promoter for expression of proteins in *Escherichia coli*. Anal. Biochem. *236*, 371–373.

Peter, M., Neiman, A.M., Park, H.O., van Lohuizen, M., and Herskowitz, I. (1996). Functional analysis of the interaction between the small GTP binding protein Cdc42 and the Ste20 protein kinase in yeast. EMBO J. *15*, 7046–7059.

Rittinger, K., Walker, P.A., Eccleston, J.F., Nurmahomed, K., Owen, D., Laue, E., Gamblin, S.J., and Smerdon, S.J. (1997). Crystal structure of a small G protein in complex with the GTPase-activating protein rhoGAP. Nature *388*, 693–697.

Sahai, E., Alberts, A.S., and Treisman, R. (1998). RhoA effector mutants reveal distinct effector pathways for cytoskeletal reorganization, SRF activation and transformation. EMBO J. *17*, 1350–1361.

Schiestl, R.H., and Gietz, R.D. (1989). High efficiency transformation of intact yeast cells using single stranded nucleic acids as a carrier. Curr. Genet. *16*, 339–346.

Schmidt, A., and Hall, M.N. (1998). Signaling to the actin cytoskeleton. Annu. Rev. Cell Dev. Biol. *14*, 305–338.

Self, A.J., Paterson, H.F., and Hall, A. (1993). Different structural organization of Ras and Rho effector domains. Oncogene *8*, 655–661.

Sherman, F., Fink, G.R., and Hicks, J.B. (1986). Methods in Yeast Genetics, Cold Spring Harbor, NY: Cold Spring Harbor Laboratory.

Shinjo, K., Koland, J.G., Hart, M.J., Narasimhan, V., Johnson, D.I., Evans, T., and Cerione, R.A. (1990). Molecular cloning of the gene for the human placental GTP-binding protein Gp (G25K): identification of this GTP-binding protein as the human homolog of the yeast cell-division-cycle protein CDC42. Proc. Natl. Acad. Sci. USA *87*, 9853–9857.

Sigal, I.S., Gibbs, J.B., D'Alonzo, J.S., and Scolnick, E.M. (1986). Identification of effector residues and a neutralizing epitope of Ha-ras-encoded p21. Proc. Natl. Acad. Sci. USA *83*, 4725–4729.

Sikorski, R.S., and Hieter, P. (1989). A system of shuttle vectors and yeast host strains designed for efficient manipulation of DNA in *Saccharomyces cerevisiae*. Genetics *122*, 19–27.

Stenmark, H., Valencia, A., Martinez, O., Ullrich, O., Goud, B., and Zerial, M. (1994). Distinct structural elements of rab5 define its functional specificity. EMBO J. *13*, 575–583.

Stevens, W.K., Vranken, W., Goudreau, N., Xiang, H., Xu, P., and Ni, F. (1999). Conformation of a Cdc42/Rac interactive binding peptide in complex with Cdc42 and analysis of the binding interface. Biochemistry *38*, 5968–5975.

Stowers, L., Yelon, D., Berg, L.J., and Chant, J. (1995). Regulation of the polarization of T cells toward antigen-presenting cells by Ras-related GTPase CDC42. Proc. Natl. Acad. Sci. USA *92*, 5027–5031.

Tjandra, H., Compton, J., and Kellogg, D. (1998). Control of mitotic events by the Cdc42 GTPase, the Clb2 cyclin and a member of the PAK kinase family. Curr. Biol. *8*, 991–1000.

Valencia, A., Chardin, P., Wittinghofer, A., and Sander, C. (1991). The *ras* protein family: evolutionary tree and role of conserved amino acids. Biochemistry *30*, 4637–4648.

Wei, Y., Zhang, Y., Derewenda, U., Liu, X., Minor, W., Nakamoto, R.K., Somlyo, A.V., Somlyo, A.P., and Derewenda, Z.S. (1997). Crystal structure of RhoA-GDP and its functional implications. Nat. Struct. Biol. *4*, 699–703.

Wertman, K.F., Drubin, D.G., and Botstein, D. (1992). Systematic mutational analysis of the yeast *ACT1* gene. Genetics *132*, 337–350.

Wu, W.J., Lin, R., Cerione, R.A., and Manor, D. (1998). Transformation activity of Cdc42 requires a region unique to Rho-related proteins. J. Biol. Chem. *273*, 16655–16658.

Xu, X., Barry, D.C., Settleman, J., Schwartz, M.A., and Bokoch, G.M. (1994). Differing structural requirements for GTPase-activating protein responsiveness and NADPH oxidase activation by Rac. J. Biol. Chem. *269*, 23569–23574.

Zerial, M., and Huber, L.A. (1995). Guidebook to the Small GTPases, New York: Sambrook and Tooze.

Zheng, Y., Cerione, R., and Bender, A. (1994). Control of the yeast bud-site assembly GTPase Cdc42: catalysis of guanine nucleotide exchange by Cdc24 and stimulation of GTPase activity by Bem3. J. Biol. Chem. *269*, 2369–2372.

Ziman, M., O'Brien, J.M., Ouellette, L.A., Church, W.R., and Johnson, D.I. (1991). Mutational analysis of *CDC42Sc*, a *Saccharomyces cerevisiae* gene that encodes a putative GTP-binding protein involved in the control of cell polarity. Mol. Cell. Biol. *11*, 3537–3544.

Ziman, M., Preuss, D., Mulholland, J., O'Brien, J.M., Botstein, D., and Johnson, D.I. (1993). Subcellular localization of Cdc42p, a *Saccharomyces cerevisiae* GTP-binding protein involved in the control of cell polarity. Mol. Biol. Cell *4*, 1307–1316.

Zohar, M., Teramoto, H., Katz, B.Z., Yamada, K.M., and Gutkind, J.S. (1998). Effector domain mutants of Rho dissociate cytoskeletal changes from nuclear signaling and cellular transformation. Oncogene *17*, 991–998.

Zohn, I.M., Campbell, S.L., Khosravi-Far, R., Rossman, K.L., and Der, C.J. (1998). Rho family proteins and Ras transformation: the RHOad less traveled gets congested. Oncogene *17*, 1415–1438.